Genome
An International Journal
for Genetics and Genomics

OPEN ACCESS | Research Article

The repetitive DNA landscape in the *brizantha* agamic complex of *Urochloa* P. Beauv.

Caio T. Rodrigues Correa[a], Magdalena Vaio[b], Sanzio C.L. Barrios[c], Cacilda B. do Valle[c], Giovana A. Torres[a], and Vânia H. Techio[a]

[a]Institute of Natural Sciences, University of Lavras, Lavras, Minas Gerais State, Brazil; [b]Facultad de Agronomía, Universidad de la República, 12900 Montevideo, Uruguay; [c]Embrapa Gado de Corte, Campo Grande, Mato Grosso do Sul State, Brazil

Corresponding author: **Vânia H. Techio** (email: vhtechio@ufla.br)

Abstract

Urochloa P. Beauv. (formerly classified as *Brachiaria* (Trin.) Griseb.) is a genus of African perennial grasses that is extensively cultivated in tropical countries for cattle nutrition. Three of the most economically relevant species, *Urochloa brizantha*, *Urochloa decumbens*, and *Urochloa ruziziensis*, form the *brizantha* agamic complex, which includes allopolyploid series with distinct subgenomes. Investigating the composition and organization of repetitive DNA, a major component of grass genomes, can provide insights into their genomic relationships and evolutionary history. This study aimed to characterize the repetitive DNA landscape of selected *Urochloa* species belonging to the *brizantha* agamic complex; identify and compare major repeat classes across species; and evaluate their potential as cytogenetic markers on mitotic chromosomes using fluorescent *in situ* hybridization (FISH). Clustering analysis revealed that repetitive DNA constitutes 56%–65% of the genomes, with Ty3/Gypsy retrotransposons, particularly the *Athila* and *Retand* lineages, representing the most abundant repeat class. *Urochloa decumbens* exhibited the highest proportion of Ty3/Gypsy retrotransposons, while *U. ruziziensis* had the highest satellite DNA content. The chromosomal location of representative satellites (UroSat-1a, UroSat-2a, and UroSat-3) was determined in all three species via FISH. UroSat-1a was detected in all centromeres, while UroSat-2a and UroSat-3 signals varied in number and position. Our findings validate the use of satDNA as cytogenetic markers in the *brizantha* agamic complex of *Urochloa* and revealed genomic relationships among different species and ploidy levels.

Key words: polyploidy, *Brachiaria*, retrotransposon, satellite DNA, tandem repeat, *in situ* hybridization

Introduction

Urochloa [Incl. *Brachiaria* (Trin.) Griseb.] is the most economically relevant genus of tropical forages, being extensively used for livestock feeding in South American countries (Jank et al. 2014). Polyploidy and hybridizations were part of the evolutionary history of *Urochloa* (Estep et al. 2014), resulting in a wide range of chromosome numbers ($2n = 14$ to 90) and ploidy levels ($2x$, $4x$, $5x$, $6x$, $7x$, $9x$) (Valle and Pagliarini 2009).

Three of the most economically important species, *Urochloa brizantha*, *U. decumbens*, and *U. ruziziensis*, form an agamic complex known as the *brizantha* complex, in which the former two are primarily apomictic tetraploids, and the latter is a sexual reproducing diploid (Lutts et al. 1991; Renvoize and Maass 1993; Renvoize et al. 1996). Polyploid series have been reported for *U. brizantha* ($2x = 18$, $4x = 36$, $5x = 45$, $6x = 54$) and *U. decumbens* ($2x = 18$, $4x = 36$, $6x = 54$), while only diploid individuals of *U. ruziziensis* ($2x = 18$) occur naturally (Valle and Pagliarini 2009; Nani et al. 2016; Corrêa et al. 2020; Moraes et al. 2021; Tomaszewska et al. 2021). Molecular phylogenies have shown that the species in the *brizantha* complex are very closely related, with an earlier speciation of *U. ruziziensis* around 5 million years ago (mya), followed by the divergence of *U. brizantha* and *U. decumbens* 1.6 mya (Pessoa-Filho et al. 2017; Triviño et al. 2017).

Extensive evidence, including meiotic studies (Mendes-Bonato et al. 2002*a*, 2002*b*, 2006; Ricci et al. 2011) and cytomolecular approaches (Paula et al. 2017; Rocha et al. 2019; Corrêa et al. 2020), has demonstrated that the tetraploidy of *U. brizantha* and *U. decumbens* had a hybrid origin. Paula et al. (2017) proposed the genomic constitution BBB^1B^1 and $B^1B^1B^2B^2$ for the allotetraploids *U. brizantha* and *U. decumbens*, respectively, and B^2B^2 for the diploid *U. ruziziensis*, using the same letter to highlight the high degree of homeology between the genomes, and the superscripts to differentiate the subgenomes. Tomaszewska et al. (2023) proposed a second genomic nomenclature, using the upper-case letters B, D, and R for *U. brizantha* (B^bB^bDD), *U. decumbens* (B^bDRR), and *U. ruziziensis* (RR), based on genome-specific repetitive DNA probes. Despite the different nomenclatures, both studies indicate that the *U. brizantha* and *U. decumbens* share subgenomes and that one of *U. decumbens* subgenomes is highly homologous with *U. ruziziensis*.

Although total genomic DNA probes can efficiently highlight homologous regions of different genomes, they cannot

Table 1. List of *Urochloa* species belonging to the *brizantha* complex, accession identitities, chromosome number, and genome size.

Species	Accession or Cultivar	Chromosome number	Genome size (Mbp)	Source
U. brizantha	B105	$2n = 2x = 18$[a]	870[a]	EMBRAPA Gado de Corte
U. brizantha	Marandu	$2n = 4x = 36$[b]	1720[c]	EMBRAPA Gado de Leite
U. decumbens	D04	$2n = 2x = 18$[a]	704[a]	EMBRAPA Gado de Corte
U. decumbens	Basilisk	$2n = 4x = 36$[b]	1855[c]	EMBRAPA Gado de Leite
U. ruziziensis	CIAT 26162	$2n = 2x = 18$[d]	732[c]	CIAT

[a]Corrêa et al. (2020).
[b]Paula et al. (2017).
[c]Penteado et al. (2000).
[d]Worthington et al. (2021).

determine the specific DNA sequences shared among them. Nonetheless, it is implied that most of the genomic differences perceived at the chromosome level are associated with the repetitive fraction of the DNA, as it can represent up to 92% of plant genomes (Fu et al. 2019). Therefore, the characterization of the repetitive genome fraction is useful to highlight overall genomic differences and similarities among closely related species. Furthermore, repetitive sequences serve as excellent chromosome markers due to their high number of copies allowing better visualization under the microscope via fluorescent in situ hybridization (FISH) (Jiang 2019).

In the *brizantha* agamic complex, the ribosomal genes 35S and 5S (Nani et al. 2016; Moraes et al. 2021), low-copy genes (Nani et al. 2018), retrotransposon lineages *CRM* (Nani et al. 2016), *Athila*, *Del*, and *Tat*, isolated from transcriptome data (Santos et al. 2015), as well as 50-mer and tandem repeats (Tomaszewska et al. 2023), have been used as probes on the agamic complex species. However, an in-depth characterization of the repeat profile across multiple species is still lacking for *Urochloa*, especially for diploid cytotypes of *U. brizantha* and *U. decumbens*.

Thus, this study aimed (i) to characterize the repetitive DNA landscape of selected *Urochloa* species belonging to the *brizantha* agamic complex; (ii) identify and compare major repeat classes across species; and (iii) evaluate the potential of satellite sequences as cytogenetic markers on mitotic chromosomes through FISH.

Materials and methods

Plant material

The studies were conducted using two diploid accessions and two tetraploid cultivars of *U. brizantha* and *U. decumbens*, as well as one diploid cultivar of *U. ruziziensis* (Table 1). Plants were cultivated in a greenhouse environment to collect material for DNA extraction and chromosome preparations.

DNA extraction and low-coverage sequencing

Genomic DNA was extracted from fresh young leaves from *U. brizantha* and *U. decumbens* accessions and cultivars using the DNEasy® Plant Mini Kit (QIAGEN Inc.). The integrity of the extracted DNA was assessed on an agarose gel 1%. The DNA was quantified and evaluated for purity (260/280 absorbance) in a Nanovue spectrophotometer (Biochrom Ltd). Genomic libraries were constructed using the Nextera™ DNA Flex Library Prep kit, with paired-end fragments of 2 × 300 bp for all samples. The libraries were sequenced using Illumina HiSeq 2500® at the Oswaldo Cruz Foundation (Fiocruz), René Rachou Institute, Belo Horizonte—MG, Brazil. The raw reads were deposited at the Sequence Read Archive (https://www.ncbi.nlm.nih.gov/sra/PRJNA1162878). Sequencing reads from *U. ruziziensis* accession CIAT 26162, obtained by Worthington et al. (2021), are available online at the European Nucleotide Archive (https://www.ebi.ac.uk/ena/browser/GCA_015476505.1) and were included in the clustering analysis.

Read processing and clustering analysis

The pre-processing of reads and clustering analysis for the identification and characterization of repetitive DNA families were performed for each accession individually using the RepeatExplorer2 pipeline (Novák et al. 2013), provided by the ELIXIR-CZ project (LM2015047), which is part of the international ELIXIR infrastructure. The reads from *U. brizantha* and *U. decumbens* were trimmed and quantity-filtered to the same length (100 bp). Low-quality reads, with 95% of bases below the cut-off phred score of 10 were discarded. The sequences were sampled to reach a genomic coverage of 0.1× so that the number of reads analyzed was proportional to the genome sizes (Table 1). After processing, the number of reads input were 435 000, 860 000, 352 000, 927 500, and 732 000 for *U. brizantha* accession B105, *U. brizantha* cultivar "Marandu", *U. decumbens* accession D04, *U. decumbens* cultivar "Basilisk", and *U. ruziziensis*, respectively.

The graph-based clustering analysis was performed with the default parameters of 90% similarity over 55% of read length. Overlapping reads were clustered, with each cluster representing a different lineage of repetitive DNA. The genomic proportion of each cluster was estimated based on the total number of reads analyzed, after the removal of plastid and mitochondrial DNA. The most representative clusters, containing ≥0.01% of the total of reads, were automatically annotated (Table S1) based on the REXdb database of plant sequences (Neumann et al. 2019). Clusters that were not automatically classified were examined for the graph layout and sequences compared against the NCBI database and GIRI RepBase databases, using the BLAST tool (Table S1).

Satellite analysis

The TAREAN (Tandem Repeat Analyzer) tool (Novák et al. 2017), also implemented on the RepeatExplorer platform, was used for identifying satellite DNA (satDNA). The similarity and identity of satellite monomers from different samples were compared via local alignment (Table S2), using the RepeatMasker platform (Smit et al. 2020). Satellites were classified according to Ruiz-Ruano et al. (2016). Satellites with >95% identity were considered the same variant; those with 80%–95% identity were considered different variants within the same family; and those with <80% identity were classified as different families. Satellite families were numbered based on their relative abundance in the genomes, with different letters used to distinguish variants within a family.

The satellite monomers were aligned with repetitive sequences previously identified in *Urochloa* species, including *U. brizantha*, *U. decumbens*, *U. humidicola*, *U. maxima*, and *U. ruziziensis* (Tomaszewska et al. 2023), and with repeats from other grass species related to *Urochloa* (Kamm et al. 1994; Ananiev et al. 1998).

Chromosome preparations and fluorescent *in situ* hybridization (FISH)

For the preparation of mitotic slides, root tips were harvested, pre-treated with cycloheximide (12.5 mg/L) for 2 h at room temperature, and fixed in an ethanol/acetic acid (3:1) solution. Cell wall digestion was performed in an enzyme solution (0.7% cellulase Onozuka R10, 0.7% cellulase Sigma–Aldrich, 1% pectolyase Sigma–Aldrich, and 1% cytohelicase Sigma–Aldrich) for 90 min at 37 °C. Slides were prepared according to the cell dissociation technique and air-dried (Dong et al. 2001).

Variants within the three satellite families with the highest genomic abundance (UroSat-1a, UroSat-2a, and UroSat-3; Supplementary Material), identified through clustering analysis, were selected for designing FISH probes. Primers were designed based on the consensus monomer sequence for each satellite variant using the online tool Primer3 (Kõressaar et al. 2018).

The genomic DNA (gDNA) was isolated from fresh leaves using the CTAB protocol (Doyle and Doyle 1990). The probes for the satellites UroSat-1a, UroSat-2a, and UroSat-3 were obtained via PCR amplification using digoxigenin-labeled nucleotides and gDNA from *U. brizantha* cultivar "Marandu", *U. decumbens* cultivar "Basilisk", and *U. decumbens* D04, respectively. PCR amplification was performed in a total volume of 25 μL containing 12.5 μL of Cellco® Taq Pol Master Mix (0.05 U/μL of Taq DNA polymerase, 0.3 mmol/L of $MgCl_2$, 0.4 mmol/L of each dNTP), 1 μL of digoxigenin-11-dUTP (0.8 mmol/L), 0.5 μL of each primer (10 μmol/L), 1 μL of DNA template (100 ng/μL), and 9.5 μL of ddH_2O. The PCR parameters were the same for all satDNA probes: an initial denaturation at 95 °C for 2 min, followed by 30 cycles of denaturation at 95 °C for 25 s, annealing at 54 °C for 1 min, and extension at 68 °C for 2 min. The integrity of the PCR products was verified by electrophoresis in an agarose gel. We also used a 35S rDNA probe (pTa71) as a positive control in the FISH assay. The 35S probe was labeled with biotin-16-dUTP via nick translation reaction.

For the FISH, chromosome slides were denatured in 70% formamide at 85 °C for 1 min and 25 s, and dehydrated in ethanol series (70%, 90%, and 100%) for 5 min each. A hybridization mixture containing 50% formamide, 10% dextran sulfate, 2× saline sodium citrate (SSC) buffer (pH 7.0), 50–100 ng of digoxigenin-labeled satellite probe, and 50–100 ng of biotin-labeled 35S rDNA probe was denatured at 95 °C and applied to the slides. The hybridization was performed in a humid chamber at 37 °C for 24 h. The hybridized slides were washed in SSC 2× for 5 min at room temperature, followed by a wash in SSC 2× at 42 °C for 10 min. The probes were detected using the antibodies anti-digoxigenin-rhodamine and Alexafluor® 488-streptavidin at 37 °C for 1 h. The chromosomes were counterstained with DAPI (4′,6-diamidino-2-phenylindole)/Vectashield® and images were captured by a QImaging Retiga EXi CCD camera attached to a fluorescence microscope Olympus BX 60. Brightness and contrast adjustments were made using Photoshop CC 2019. The number and position of UroSat-1a, UroSat-2a, and UroSat-3 sites were determined by analyzing a minimum of 10 selected metaphases across at least three slides per accession.

Results

Genomic proportions of repetitive DNA classes

The estimated repetitive DNA proportion ranged from 56.26% in *Urochloa brizantha* 2*x* to 65.52% in *U. brizantha* 4*x* (Table 2). In the diploid cytotype of *U. brizantha*, 250 665 reads were classified as repetitive DNA, grouped into 35 764 clusters, of which 316 were considered the most representative (top clusters) for containing at least 0.01% of the total sequences each. The tetraploid cytotype displayed 573 645 reads, grouped into 69 042 clusters, with 263 top clusters. In the diploid cytotype of *U. decumbens*, 224 715 reads represented repetitive DNA, grouped into 24 208 clusters and 267 top clusters. The tetraploid cytotype had 610 784 repetitive reads, in 71 403 clusters and 259 top clusters. In *U. ruziziensis*, 442 300 reads were grouped into 36 854 clusters and 249 top clusters.

Transposable elements

The annotated proportions of repetitive DNA of the analyzed species are displayed in Table 2 and Figs. 1 and 2. Long-terminal repeat (LTR) retrotransposons are the most common repetitive element in the *Urochloa* genomes (23.5%–34%). The most frequent LTR superfamily was *Ty3*/*Gypsy* (16.8%–23.9%) and the percentages of the different repeat families within *Ty3*/*Gypsy* varied among the three species (Fig. 2A). In *U. brizantha* and *U. decumbens*, *Athila* was the most frequent *Gypsy* lineage, followed by *Retand* and *Tekay*. In *U. ruziziensis*, *Retand*, and *Athila* had similarly high proportions.

Urochloa brizantha had a larger fraction of *Ogre* elements, while *U. decumbens* 2*x* and *U. ruziziensis* 2*x* had noticeably lower proportions. Transposable elements classified as CRMs (Centromeric Repeats, originally identified in maize) were also present in all genomes, being more frequent in the diploids.

Table 2. Genomic proportions (%) of repeat classes and families in *Urochloa brizantha* diploid (UB2) and tetraploid (UB4), *U. decumbens* diploid (UD2) and tetraploid (UD4), and *U. ruziziensis* (UR).

		UB2	UB4	UD2	UD4	UR
Class I retroelements	Lineage					
LTR	(unclassified)	1.69	2.52	0.41	1.27	3.25
Ty1/Copia	(unclassified)	0.71	0.55	1.11	0.28	0.42
	Ale	0.08	0.21	0.05	0.11	0.08
	Angela	0.19	0.26	0.15	0.29	0.17
	Bianca	0.15	0.27	0.08	0.25	0.00
	Ikeros	0.42	0.66	0.59	0.69	0.59
	SIRE	4.88	6.82	7.84	7.16	9.47
	TAR	0.16	0.32	0.21	0.28	0.21
	Tork	0.06	0.07	0.05	0.30	0.08
Total *Ty1/Copia*		6.65	9.16	10.08	9.36	11.02
Ty3/Gypsy	(unclassified)	4.45	2.53	2.10	1.51	1.13
	Athila	3.73	5.74	7.39	7.60	5.70
	CRM	0.95	0.63	1.27	0.76	1.44
	Ogre	2.37	2.33	0.48	1.66	0.46
	Reina	0.08	0.00	0.03	0.05	0.00
	Retand	3.50	5.03	7.11	5.48	5.93
	Tekay	1.74	3.30	5.49	4.89	3.88
Total *Ty3/Gypsy*		16.82	19.56	23.87	21.95	18.54
Total LTR		25.16	31.24	34.36	32.58	32.81
Other	LINE	0.05	0.12	0.09	0.45	0.10
	SINE	0.04	0.05	0.00	0.04	0.07
	MITE	0.02	0.03	0.00	0.02	0.00
	Caulimovirus	0.05	0.13	0.00	0.02	0.00
Total retrotransposons		25.32	31.57	34.45	33.11	32.98
Class II	(unclassified)	0.00	0.00	0.03	0.09	0.05
DNA transposons	CACTA	1.76	3.22	2.29	3.10	2.05
	hAT	0.02	0.12	0.25	0.10	0.18
	Mutator	0.16	0.41	0.42	0.34	0.29
	Harbinger	0.26	0.43	0.52	0.48	0.55
	Mariner	0.13	0.37	0.18	0.17	0.25
	Helitron	0.02	0.13	0.02	0.01	0.22
Total DNA transposons		2.35	4.68	3.71	4.29	3.59
Tandem repeats						
	Satellites	3.86	3.83	2.62	2.97	4.65
	rDNA	1.25	1.85	2.30	1.50	0.90
Total tandem repeats		5.11	5.68	4.92	4.47	5.55
Annotated repeats		32.78	41.93	43.08	41.87	42.12
Total repetitive DNA		56.26	65.52	62.48	64.78	57.75

Note: LTR, long-terminal repeat.

The second most abundant superfamily of LTRs was *Ty1/Copia* (6.6%–11%). Among *Ty1/Copia* elements (Fig. 2B), Sireviruses (SIRE) were much more frequent than other lineages, being especially high in *U. ruziziensis*. The percentages of *Bianca* and *Angela* retrotransposons were higher in the tetraploid cytotypes of both species. The tetraploid cytotype of *U. decumbens* had six-fold more *Tork* elements than the other samples.

DNA transposons represented 2.4%–4.7% of the genomes analyzed (Table 2). *CACTA* was the most common transposon superfamily in all *Urochloa* species, seemingly higher in tetraploids, followed by *Harbinger* and *Mutator* (Fig. 2C). The number of *Helitron* and*Mariner* repeats were especially larger in *U. brizantha* 4*x* and *U. ruziziensis* 2*x*, while *hAT* elements were more frequent in *U. decumbens* 4*x* and *U. ruziziensis* 2*x*.

Satellite DNA

Tandem repeats were mainly represented by ribosomal genes (1.2%–2.3%) and satellite DNA (2.6%–4.6%; Table 2). Eleven satellite DNA families were identified based on local alignments, three of which (UroSat-1, UroSat-2, and UroSat-6) exhibited different variants. The lengths of satellite

Fig. 1. Repetitive fraction of *Urochloa* genomes showing relative abundance of DNA transposons, *Copia* and *Gypsy* retrotransposons, rDNA, satellite DNA, and unclassified repeats. UB2: *Urochloa brizantha*, diploid; UB4: *Urochloa brizantha*, tetraploid; UD2: *U. decumbens*, diploid; UD4: *U. decumbens*, tetraploid. UR: *U. ruziziensis*.

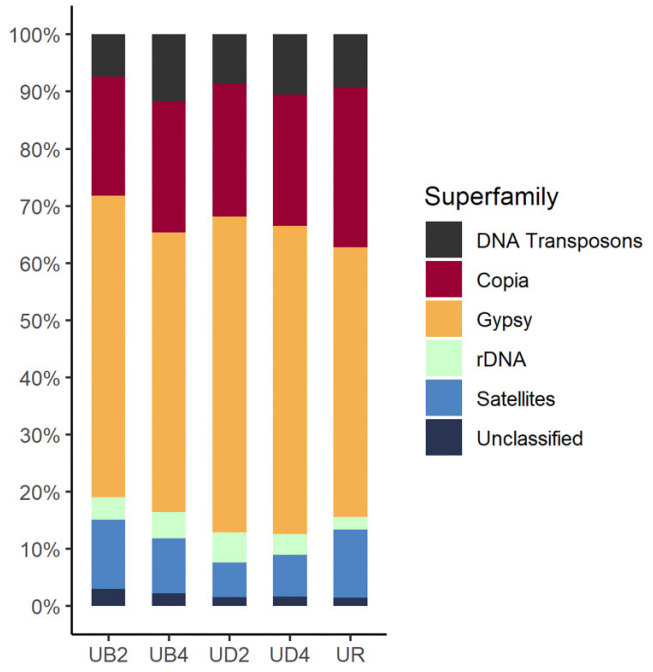

monomers ranged from 78 to 744 bp, with 158 and 360–380 bp being the most common (Table S3). The A-T content was similar within the satellite families, with an average of 56.6% (Table S3).

Urochloa brizantha had a higher number and proportion of satellites than *U. decumbens* (Table 2, Fig. 3). In *U. brizantha*, all 11 satellite families identified were present, with 14 variants identified in both cytotypes, and 10 variants shared between them. Four exclusive satellites were found in *U. brizantha* 2*x*, while one was found in *U. brizantha* 4*x*. In *U. decumbens*, only three satellite families were identified in the diploid cytotype (UroSat-1, UroSat-3, and UroSat-8), all shared with *U. decumbens* 4*x*, which had a total of seven DNA satellites families. *Urochloa ruziziensis* exhibited the smallest number and largest proportion of satellites among the three species. The satellites found in *U. ruziziensis* (UroSat-1a, UroSat-3, and UroSat-8) were the same ones found in *U. decumbens* 2*x*, which were shared among the three species.

Satellite variants were only observed for UroSat-1, UroSat-2, and UroSat-6. UroSat-1 was the most diverse family of satDNA, including six variants. Four of these variants (UroSat-1c, UroSat-1d, UroSat-1e, and UroSat-1f) were unique to *U. brizantha*, three of which were exclusive to diploid cytotype.

The comparison of the identified satellite monomers with tandem repeats previously reported for *Urochloa* revealed that nine variants were highly similar to 21 repeats from *U. brizantha*, *U. decumbens*, and *U. humidicola* (Table 3). Alignment identities ranged from 81.82% to 100% over query coverages of 28%–100%. UroSat-1a (158 bp) was also related to centromeric satellites from maize, *Cenchrus americanus* and *Tripsacum dactyloides*.

Fluorescent *in situ* hybridization

The probing of satellite DNA successfully revealed the organization of UroSat-1a, UroSat-2a, and UroSat-3 on *Urochloa* chromosomes (Fig. 4, Table 4). None of the probed satellites overlapped with rDNA 35S sites in any species. UroSat-1a was detected in the centromeric region of all chromosomes of all species and cytotypes evaluated (Figs. 4A–4E). The UroSat-2a probe produced signals located on terminal regions of the chromosomes (Figs. 4F–4L), while the location of UroSat-3 varied among the terminal region of short arms, long arms, or both arms (Figs. 4M–4P). UroSat-2a was present as strong and well-defined bands in *U. brizantha* 2*x* and 4*x* (Figs. 4F and 4G), and *U. decumbens* 4*x* (Fig. 4H), and as unspecific weaker signals in *U. decumbens* 2*x* and *U. ruziziensis* (Figs. 4I–4L). UroSat-3 was present in all species and cytotypes, apart from *U. brizantha* 2*x*.

In *U. brizantha*, three pairs of UroSat-2a signals were observed in the diploid form (Fig. 4F), while the tetraploid form presented four (Fig. 4G). UroSat-3 was found on six chromosome pairs in *U. brizantha* 4*x*, and it was hemizygous in the pair bearing the rDNA 35S site (Fig. 4M). This probe did not produce any signals on the diploid cytotype of this species.

In *U. decumbens*, UroSat-3 signals were found in all chromosomes of the diploid cytotype (Fig. 4N), including the pair containing the 35S rDNA site. The same probe produced signals on ten chromosome pairs of *U. decumbens* 4*x* (Fig. 4O). In the tetraploid *U. decumbens*, one of the chromosome pairs containing the 35S rDNA site exhibited a heteromorphic tertiary constriction associated with an UroSat-2a signal (Fig. 4H). Signals were also found on four other chromosomes. UroSat-2 signals were variable and inconsistent in terms of number and location in *U. decumbens* 2*x* (Figs. 4I and 4J), therefore it was not possible to assign them to specific chromosome pairs.

In *U. ruziziensis*, UroSat-3 signals were observed on all chromosomes except for the pair containing the 35S rDNA site (Fig. 4P). As in *U. decumbens* 2*x*, the UroSat-2 probe produced inconsistent FISH signals, displaying weak intensity and variable numbers of signals across different assays (Figs. 4K and 4L).

Discussion

Repetitive DNA composition

Repetitive DNA is the main component of *Urochloa* genomes, which is consistent with what has been reported for other cultivated grasses, like maize (70%–80%), wheat (~80%), and barley (~85%) (Meyers et al. 2001; Garbus et al. 2015; Wicker et al. 2017). Overall, the total proportions of the major repeat classes (retrotransposons, transposons, and tandem repeats) were similar among all genomes, except for the diploid cytotype of *U. brizantha*, which exhibited lower percentages for all classes. *Urochloa brizantha* 2*x* also displayed a larger proportion of transposable elements unidentified by repeat databases, thereby having a more diverse repeat profile.

Fig. 2. Genomic proportions of different lineages of *Gypsy* retrotransposons (A), *Copia* retrotransposons (B), and DNA transposons (C) in *Urochloa* genomes.

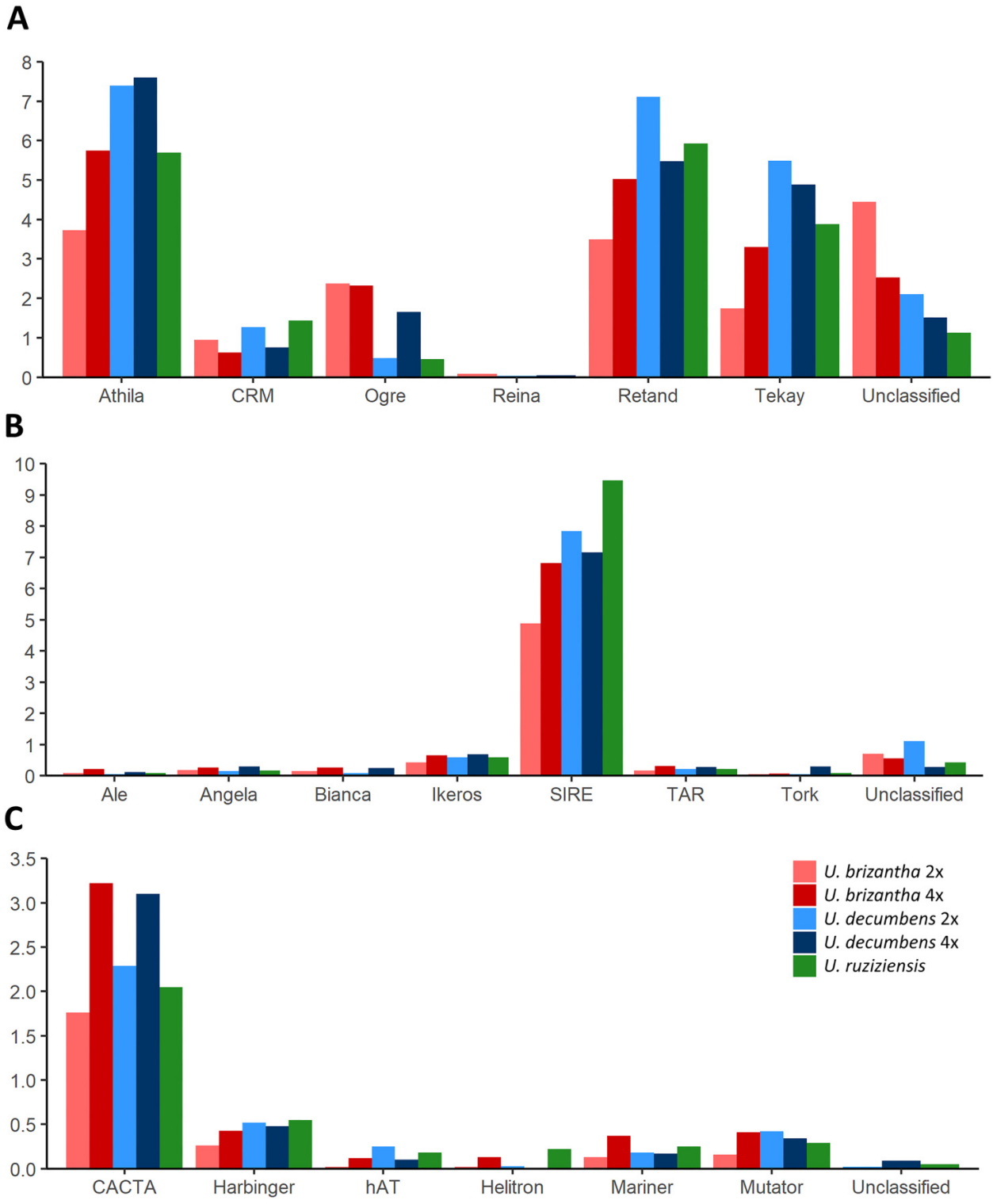

The genomic proportion of LTR retrotransposons was previously reported for *U. ruziziensis* at 33.5% in a study focused on QTL mapping for aluminum tolerance genes (Worthington et al. 2021), which is consistent with our estimate for this species (32.98%). However, the proportions of *Gypsy* and *Copia* elements in our analysis (18.54% and 11.05%, respectively) differed from the values reported by Worthington et al. (2021), which were 24% *Gypsy* and 9.5% *Copia*. These discrepancies may be due to the different methodologies used for LTR identification, as we used the RepeatExplorer

Fig. 3. Genomic proportion of satellite DNA families in *Urochloa* species. The size of the circles corresponds to the relative abundance of the satellite families in each genome. Numbers above the circles indicate the genomic proportion of each satellite variant. *Urochloa brizantha* 2*x* (UB2), *U. brizantha* 4*x* (UB4), *U. decumbens* 2*x* (UD2), *U. decumbens* 4*x* (UD4), and *U. ruziziensis* 2*x* (UR).

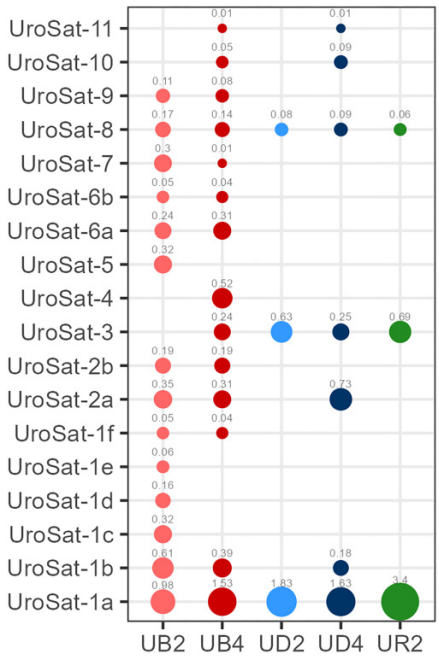

pipeline (Novák et al. 2013) and Worthington et al. (2021) used the software LTRharvest (Ellinghaus et al. 2008).

Retrotransposon activity has been attributed as the main driver of genome size increases in grasses, as the copy-and-paste transposition mechanism of these elements can lead to the rapid accumulation of repeats (Vicient et al. 2001). This seems to be valid for the *brizantha* agamic complex of *Urochloa*, considering that most of the repeats identified in this study are LTR retrotransposons, predominantly *Gypsy* elements. In addition to the large genomic proportion of *Gypsy* LTRs, RNA sequencing data have shown that they also represented near half of the transcriptome of *U. decumbens* 4*x* (Santos et al. 2015).

Athila elements, the most abundant *Gypsy* lineage identified in our study, have previously shown high expression levels in *Urochloa*, and are associated with centromeric and pericentromeric regions of all chromosomes in *U. brizantha* 4*x*, *U. decumbens* 2*x*, and *U. ruziziensis*, as revealed by FISH probing (Santos et al. 2015). *Tat* and CRM elements have also been mapped to *Urochloa* chromosomes, with the former being scattered throughout interstitial regions and the latter located in the centromere, although a few chromosomes of *U. brizantha* 4*x* and *U. decumbens* 2*x* lacked the signal (Santos et al. 2015; Nani et al. 2016). Other *Gypsy* elements previously reported in *U. decumbens* transcriptome (Santos et al. 2015), such as *Del* and *Galadriel*, were not identified in our study, but they may be present in low proportions, as repeats below the 0.01% threshold were not annotated.

The *Copia* superfamily was mainly composed of *Sirevirus* (SIRE), an ancient plant-specific retrotransposon lineage, which was also the most frequent LTR in *Urochloa*. These elements are highly conserved across the plant kingdom and have been found in many grass species, including rice, sorghum, and maize, in which they occupy 21% of the genome (Bousios et al. 2012).

DNA transposons were predominantly represented by *CACTA* elements, which accounted for a four-fold larger proportion compared to other repeats. The *CACTA* superfamily, named after the terminal inverted repeat sequence that flanks these elements, is a diverse group of transposons, including several lineages, such as *CAC1* from *Arabidopsis thaliana*, *Caspar* from Triticeae, and *En/Spm* from maize (Gierl 1996; Miura et al. 2001; Wicker et al. 2003). All the *CACTA* repeats identified in our study were related to maize's *En/Spm* lineage, which suggests the conservation of these elements in the Panicoideae subfamily.

By using local alignment matrices, we were able to distinguish 11 satellite families for *U. brizantha*, *U. decumbens* and *U. ruziziensis*. The occurrence of UroSat-1, UroSat-3, and UroSat-8 in the three species suggests that these variants are more ancestral than the other satellites, likely having originated prior to speciation events. Additionally, the high sequence identity of the UroSat-1a across the different *Urochloa* species is possibly due to its conserved centromeric role. This is also supported by the high sequence similarity between UroSat-1a and centromeric repeats from other grass species, such as maize (Ananiev et al. 1998) and *Cenchrus americanus* (Kamm et al. 1994).

Urochloa brizantha and *U. decumbens* shared more satellites with each other than with *U. ruziziensis*. This finding corroborates the most recent phylogenetic analysis for *Urochloa* that traced the divergence between *U. ruziziensis* and the other two species to 5.6 million years ago, followed by a more recent divergence between *U. brizantha* and *U. decumbens* around 1.6 mya (Pessoa-Filho et al. 2017). The larger number of satellites and the occurrence of species-specific satellites in *U. brizantha* (UroSat-1f, 2b, 6a, 6b, 7, and 9) indicates that its divergence from *U. decumbens* was accompanied by a great diversification of tandem repeats. This repeat diversity is more apparent when comparing the diploid cytotype of *U. brizantha*, which has four exclusive satellites (UroSat-1c, 1d, 1e, and 5), to *U. decumbens* 2*x* and *U. ruziziensis*, which each have only three non-exclusive satellites. The higher diversity in *U. brizantha* 2*x* had already been indicated by the reciprocal GISH performed on the diploid cytotypes (Corrêa et al. 2020), where its genomic probe fully hybridized with all chromosomes of *U. decumbens* 2*x*, while the opposite probing produced only ~65% of hybridization.

Chromosomal location of satellite sequences

The physical location of the probed satellite sequences on the *Urochloa* species studied was consistent with the satellitome characterized in silico: UroSat-1a was detected in all species and cytotypes, UroSat-3 was absent in *U. brizantha* 2*x*, but present in the other cytotypes and species, and UroSat-2a was observed only in *U. brizantha* (2*x* and 4*x*), and

Table 3. Alignments between the identified *Urochloa* DNA satellite sequences (UroSat) and previously reported tandem repeats.

Satellite	Length (bp)	Reported Id. repeat	Length (bp)	Species	Query coverage (%)[a]	Identity (%)[b]
UroSat-1a	158	TCL2[c]	158	*Urochloa brizantha*	92	98.63
		CL1[c]	158	*U. decumbens*	83	100.00
		TCL12[c]	158	*U. brizantha*	93	100.00
		CL1[c]	158	*U. brizantha*	98	98.02
		CL4[c]	158	*U. brizantha*	98	97.50
		CL100[c]	567	*U. humidicola*	68	91.74
		Sat-1 A[d]	70	*Cenchrus americanus*	38	81.82
		CentT57[e]	156	*Tripsacum dactyloides*	82	91.60
		Cent-C-158a[f]	158	*Zea mays*	46	75.68
UroSat-1b	158	CL67[c]	158	*U. decumbens*	100	98.37
		CL44[c]	158	*U. brizantha*	100	98.46
		CL9[c]	157	*U. brizantha*	100	98.36
		TCL2[c]	158	*U. brizantha*	59	91.49
UroSat-1e	314	CL121[c]	157	*U. brizantha*	75	93.08
		CL72[c]	154	*U. humidicola*	46	90.67
		CL9[c]	157	*U. humidicola*	28	84.62
UroSat-1f	158	CL9[c]	158	*U. brizantha*	96	90.79
UroSat-2a	361	CL34[c]	361	*U. brizantha*	77	95.36
UroSat-2b	362	CL35[c]	362	*U. brizantha*	98	96.83
UroSat-7	566	CL100[c]	156	*U. brizantha*	100	99.54
UroSat-8	740	CL101[c]	761	*U. decumbens*	99	94.90
		CL77[c]	744	*U. brizantha*	100	100.00
UroSat-9	498	CL83[c]	418	*U. brizantha*	82	94.83

[a]Query coverage indicates the proportion of the sequence included in the alignment.
[b]Identity indicates the proportion of identical bases.
[c]Tomaszewska et al. (2023).
[d]Kamm et al. (1994).
[e]Melo and Dawe (2004).
[f]Ananiev et al. (1998).

U. decumbens 4*x*. However, we observed highly variable and unspecific UroSat-2a signals in *U. decumbens* 2*x* and *U. ruziziensis*, where this sequence had not been identified in silico. These signals may have been produced by probes binding to degraded DNA segments with some degree of homology with the satellite sequence, as often occurs with FISH probing (Wang et al. 2001; Jiang 2019).

The probing of UroSat-2a allowed the differentiation of three chromosome pairs in *U. brizantha* 2*x*, four pairs in *U. brizantha* 4*x*, and three pairs in *U. decumbens* 4*x*. The disproportional number of sites between the diploid and tetraploid cytotypes of *U. brizantha* and *U. decumbens* may be a consequence of the allopolyploidization and diploidization events involving these two species. Such variation has also been observed for 35S and 5S rDNA sites in previous studies (Akiyama et al. 2010; Nani et al. 2016).

The heteromorphic tertiary constriction observed in *U. decumbens* 4*x* was previously reported by Nani et al. (2016). Our FISH results further demonstrate that satellite DNA is a major component of this structure, as evidenced by its colocalization with UroSat-2a. Tertiary constrictions have been reported in other grass species, such as barley (Gecheff 1976), rye (Jenkins et al. 2005), gamagrass (Koo and Jiang 2008), often associated with chromosomal breaks. Tandem repeats are also considered frequent breakage sites and hotspots for chromosome rearrangements (Arlt et al. 2006), therefore, the presence of UroSat-2a at this site could be contributing to the formation of the tertiary constriction.

The presence of UroSat-1a exclusively on the centromeric region of chromosomes in all the genotypes suggests that this sequence is an essential component of *Urochloa* centromeres. Satellite DNA is a common constituent of plant centromeres, and several centromeric satellites have been identified in grass species, such as maize, wheat, and oat (Jin et al. 2004; Oliveira and Torres 2018; Su et al. 2019). Additional evidence supporting the centromeric role of UroSat-1a is the high level of conservation of this satellite among *Urochloa* species, with 100% sequence identity among satellites independently identified via bioinformatic analysis in *U. brizantha*, *U. decumbens*, and *U. ruziziensis*, as well as the high similarity between UroSat-1a and centromeric satellites from maize (~75%) and *Cenchrus americanus* (~82%). This high conservation of centromeric satellites among grasses has also been demonstrated in comparative analysis involving different species, including barley, rice, maize, millet, and *Panicum* (Melters et al. 2013).

The centromeric role of UroSat-1a is likely extended to other *Urochloa* species beyond the *brizantha* agamic complex,

Fig. 4. Fluorescent *in situ* hybridization (FISH) probing of satellite DNAs UroSat-1a (pink), UroSat-2a (red), UroSat-3 (blue), and 35S rDNA (green) on metaphase chromosomes of *Urochloa brizantha* diploid $2n = 18$ (A, F) and tetraploid $2n = 36$ (B, G), *U. decumbens* diploid $2n = 18$ (C, I, J, N) and tetraploid $2n = 36$ (D, H, O), and *U. ruziziensis* diploid $2n = 18$ (E, K, L). Yellow arrows indicate a tertiary constriction on a chromosome in *U. decumbens* 4*x*. A magnified view of this chromosome is provided on the top left of panels D and H.

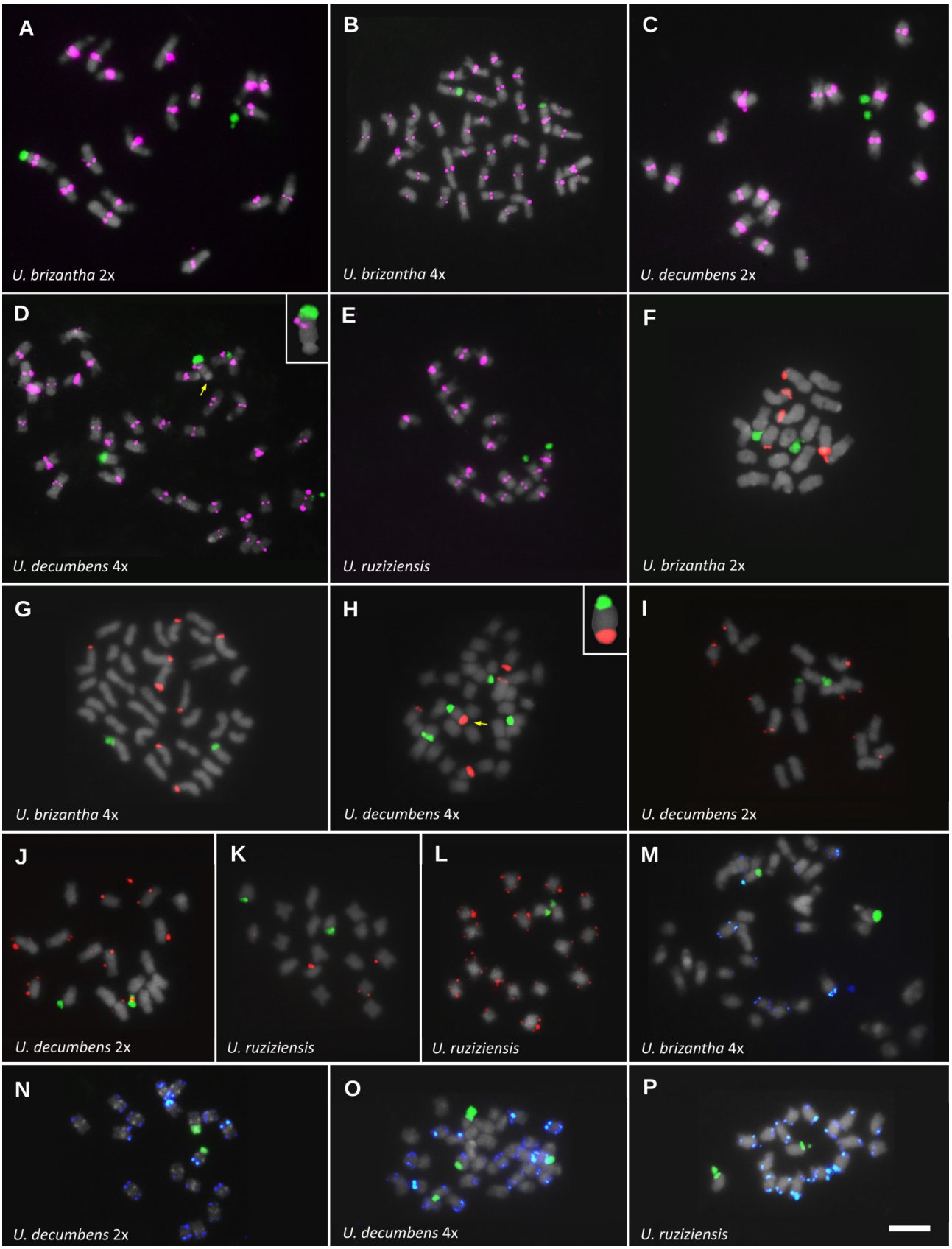

Table 4. Number and chromosomal positions of fluorescent *in situ* hybridization (FISH) signals for the satellite sequences UroSat-1a, UroSat-2a, and UroSat-3 in *Urochloa*.

Species	UroSat-1a	UroSat-2a	UroSat-3
U. brizantha 2*x*	18 C	3 TS	no signals
U. brizantha 4*x*	36 C	4 TS	4 TSL + 2 TS + 1 TL*
U. decumbens 2*x*	18 C	unspecific signals	5 TSL + 3 TS + 1 TL
U. decumbens 4*x*	36 C	2 TS + 1 TL	7 TSL + 2 TS + 1 TL
U. ruziziensis 2*x*	18 C	unspecific signals	6 TSL + 2 TS

Note: Signals were found on centromeric (C) and terminal (T) regions of short arms (S) and long arms (L).
*Heteromorphic pair.

as it is highly similar (92% identity) to a tandem repeat (CL100) identified in an accession of *U. humidicola* in a different study (Tomaszewska et al. 2023). However, the repeat was not mapped to *U. humidicola* chromosomes, thereby its physical location is yet to be confirmed. Nonetheless, our findings for UroSat-1a enable its use as a FISH probe in several applications, such as karyotype descriptions, characterization of centromeres, tracking chromosome breaks and rearrangements, comparative cytogenetic analyses, and studies on chromosome evolution.

The distribution of UroSat-3 signals is consistent across *U. decumbens* 2*x*, 4*x*, *U. ruziziensis*, and tetraploid *U. brizantha*, highlighting shared repetitive sequences among these cytotypes, which is consistent with the data from the clustering analysis and with *in situ* hybridization studies (Corrêa et al. 2020; Tomaszewska et al. 2023). In contrast, the absence of UroSat-3 in diploid *U. brizantha* points to a pre-speciation origin of this satellite and its subsequent elimination in the diploid lineage.

Allopolyploidization models and satellite DNA composition in the *brizantha* complex

The characterization of satellite DNA composition provided insights into the genomic relationships of the species in the *brizantha* agamic complex. Both allopolyploidization models proposed for the group suggest that tetraploids *U. brizantha* (BBB^1B^1) and *U. decumbens* ($B^1B^1B^2B^2$) share a subgenome likely inherited from a diploid *U. decumbens* parent (Paula et al. 2017; Tomaszewska et al. 2023). In this scenario, the two satellites found exclusively in the tetraploids (UroSat-10 and UroSat-11) may be associated with this subgenome (B^1B^1). This is further supported by the chromosomal locations of UroSat-2a and UroSat-3, which were more similar between the tetraploid cytotypes of *U. brizantha* and *U. decumbens* than between their diploid counterparts. These patterns align with the genetic structure of the *brizantha* agamic complex reported by Higgins et al. (2022), which showed that tetraploid accessions of *U. brizantha* and *U. decumbens* are phylogenetically closer to each other than to their diploid relatives due to the reproductive barriers caused by polyploidization events. This finding supported the hypothesis that a single polyploidization event established both tetraploid *U. brizantha* and *U. decumbens* (Higgins et al. 2022), which is consistent with previous evolutionary models proposed for the *brizantha* complex (Pessoa-Filho et al. 2017; Tomaszewska et al. 2023) and corroborated by our results.

The diploid cytotype of *U. brizantha* was initially associated with the genome B^1B^1 due to the similar hybridization patterns of its genomic DNA on both *U. brizantha* 4*x* (BBB^1B^1) and *U. decumbens* 4*x* ($B^1B^1B^2B^2$) via GISH probing (Corrêa et al. 2020). However, most of the satellite families found in *U. brizantha* 2*x* were not present in *U. decumbens* 4*x*, indicating that the homologous regions highlighted by the GISH may be mostly due to the high TE composition. Post-polyploidization genomic rearrangements may have also affected the satellitome of *U. decumbens*, leading to the elimination of parental sequences. Nonetheless, the occurrence of six species-specific satellites in *U. brizantha* indicates that the diploid cytotype is indeed close to one of the subgenomes of its tetraploid counterpart.

The genome B^2, identified in *U. ruziziensis,* could not be distinguished by the satellite composition, since the only three satellites detected in this species (UroSat-1a, UroSat-3 and UroSat-8) were shared among all species. However, chromosome markers for this genome could still be developed through the use of TE probes, as well as though the physical mapping of UroSat-8, which may present different FISH patterns across species.

Conclusions

The composition and chromosomal organization of repetitive DNA in the *brizantha* agamic complex of *Urochloa* reflect the hybridization and polyploidy history of the species involved, with patterns shaped by ploidy and phylogeny.

We were able to determine that genomes in the *brizantha* agamic complex of *Urochloa* are primarily composed of repetitive DNA, with *Gypsy* retrotransposons being the most representative repeat lineage. Some satellite DNA families were highly conserved across species, such as UroSat-1 and UroSat-8, while others were present only in individuals within the same species or ploidy level. These distribution patterns are useful for comparative cytogenetics studies in which satellite sequences can serve as probes, as we were able to demonstrate with UroSat-1a, UroSat-2a, and UroSat-3.

Acknowledgements

We would like to thank the Coordination for the Improvement of Higher Education Personnel (CAPES), the National Council for Scientific and Technological Development (CNPq), and the Research Foundation of the State of Minas

Gerais (FAPEMIG) for funding this project. The CNPq for providing the PhD scholarships and the Oswaldo Cruz Foundation (Fiocruz) for genome sequencing.

Article information

History dates

Received: 8 July 2024
Accepted: 6 January 2025
Accepted manuscript online: 31 January 2025
Version of record online: 25 April 2025

Notes

This paper is part of a collection entitled "Cytogenomics: Exploring Chromosome Structure and Function." https://cdnsciencepub.com/topic/gen-cytogenomics_chromsome_structure_function.

Copyright

Data availability

All data supporting the findings of this study are available within the paper and its Supplementary Information.

Author information

Author ORCIDs

Vânia H. Techio https://orcid.org/0000-0002-3752-0654

Author contributions

Conceptualization: GAT, VHT
Formal analysis: CTRC
Funding acquisition: VHT
Investigation: CTRC
Methodology: CTRC, MV, GAT
Project administration: VHT
Resources: SCLB, CBdV, GAT, VHT
Supervision: VHT
Writing – original draft: CTRC
Writing – review & editing: CTRC, MV, SCLB, CBdV, GAT, VHT

Competing interests

The authors declare no conflicts of interest.

Funding information

This research was supported by the Conselho Nacional de Desenvolvimento Científico e Tecnológico (National Council for Scientific and Technological Development—CNPq—307912/2022-1), Coordenação de Aperfeiçoamento de Pessoal de Nível Superior (Coordination for the Improvement of Higher Education Personnel—CAPES) and the Research Foundation of the State of Minas Gerais (FAPEMIG—PPM-00259-17)

Supplementary material

Supplementary data are available with the article at https://doi.org/10.1139/gen-2024-0096.

References

Akiyama, Y., Yamada-Akiyama, H., and Ebina, M. 2010. Morphological diversity of chromosomes bearing ribosomal DNA loci in Brachiaria species. Grassl. Sci. **56**: 217–223. doi:10.1111/j.1744-697X.2010.00197.x.

Ananiev, E.V., Phillips, R.L., and Rines, H.W. 1998. Chromosome-specific molecular organization of maize (*Zea mays* L.) centromeric regions. Proc. Natl. Acad. Sci. U S A **95**: 13073–13078. doi:10.1073/pnas.95.22.13073. PMID: 9789043.

Arlt, M.F., Durkin, S.G., Ragland, R.L., and Glover, T.W. 2006. Common fragile sites as targets for chromosome rearrangements. DNA Repair, **5**: 1126–1135. doi:10.1186/s13578-020-00392-5. PMID: 16807141.

Bousios, A., Minga, E., Kalitsou, N., Pantermali, M., Tsaballa, A., and Darzentas, N. 2012. MASiVEdb: the Sirevirus Plant retrotransposon Database. BMC Genomics, **13**: 1–10. Available at:. doi:10.1186/1471-2164-13-158. PMID: 22214261.

Corrêa, C.T.R., Bonetti, N.G.Z., Barrios, S.C.L., do Valle, C.B., Torres, G.A., and Techio, V.H. 2020. GISH-based comparative genomic analysis in *Urochloa* P. Beauv. Mol. Biol. Rep. **47**: 887–896. Available at:. doi:10.1007/s11033-019-05179-7. PMID: 31734896.

Dong, F., McGrath, J.M., Helgeson, J.P., and Jiang, J. 2001. The genetic identity of alien chromosomes in potato breeding lines revealed by sequential GISH and FISH analyses using chromosome-specific cytogenetic DNA markers. Genome, **44**: 729–734, Available at:. doi:10.1139/gen-44-4-729.

Doyle, J., and Doyle, J.L. 1990. Isolation of plant DNA from fresh tissue. Focus, **12**: 39–40.

Ellinghaus, D., Kurtz, S., and Willhoeft, U. 2008. LTRharvest, an efficient and flexible software for de novo detection of LTR retrotransposons. BMC Bioinformatics, **9**: 1–14. doi:10.1186/1471-2105-9-18. PMID: 18173834.

Estep, M.C., Mckain, M.R., Vela Diaz, D., Zhong, J., Hodge, J.G., Hodkinson, T.R., et al. 2014. Allopolyploidy, diversification, and the Miocene grassland expansion. Proc. Natl. Acad. Sci. **111**: 15149–15154. doi:10.1073/pnas.1404177111.

Fu, J., Zhang, H., Guo, F., Ma, L.u, Wu, J., Yue, M., et al. 2019. Identification and characterization of abundant repetitive sequences in *Allium cepa*. Sci. Rep. **9**: 1–13. doi:10.1038/s41598-019-52995-9. PMID: 30626917.

Garbus, I., Romero, J.R., Valarik, M., Vanžurová, H., Karafiátová, M., Cáccamo, M., et al. 2015. Characterization of repetitive DNA landscape in wheat homeologous group 4 chromosomes. BMC Genomics, **16**: 1–10. doi:10.1186/s12864-015-1579-0. PMID: 25553907.

Gecheff, K.I. 1976. A new translocation in barley resulting in a cytologically marked karyotype. Mutation Research/Fundamental and Molecular Mechanisms of Mutagenesis, **36**: 241–244. doi:10.1016/0027-5107(76)90011-7.

Gierl, A. 1996. The En/Spm transposable element of maize. In: Transposable elements. Springer, pp. 145–159.

Higgins, J., Tomaszewska, P., Pellny, T.K., Castiblanco, V., Arango, J., Tohme, J., et al. 2022. Diverged subpopulations in tropical *Urochloa* (Brachiaria) forage species indicate a role for facultative apomixis and varying ploidy in their population structure and evolution. Ann. Bot. **130**(5): 657–669. doi:10.1093/aob/mcac115. PMID: 36112370.

Jank, L., Barrios, S.C., Do Valle, C.B., Simeão, R.M., and Alves, G.F. 2014. The value of improved pastures to Brazilian beef production. Crop Pasture Sci. **65**: 1132–1137. doi:10.1071/CP13319.

Jenkins, G., Mikhailova, E.I., Langdon, T., Tikholiz, O.A., Sosnikhina, S.P., and Jones, R.N. 2005. Strategies for the study of meiosis in rye. Cytogenet. Genome Res. **109**: 221–227. doi:10.1159/000082404. PMID: 15753581.

Jiang, J. 2019. Fluorescence in situ hybridization in plants: recent developments and future applications. Chromosome Res. **27**: 153–165. doi:10.1007/s10577-019-09607-z. PMID: 30852707.

Jin, W., Melo, JR., Nagaki, K., Talbert, PB., Henikoff, S., Dawe, R.K, and Jiang, J. 2004. Maize centromeres: organization and functional

adaptation in the genetic background of oat. Plant Cell, **16**: 571–581. doi:10.1105/tpc.018937.

Kamm, A., Schmidt, T., and Heslop-Harrison, J.S. 1994. Molecular and physical organization of highly repetitive, undermethylated DNA from *Pennisetum glaucum*. Mol. Gen. Genet. MGG, **244**: 420–425. Available at:. doi:10.1007/BF00286694.

Koo, D.H., and Jiang, J. 2008. Extraordinary tertiary constrictions of *Tripsacum dactyloides* chromosomes: implications for karyotype evolution of polyploids driven by segmental chromosome losses. Genetics, **179**: 1119–1123. Available at:. doi:10.1534/genetics.108.087726. PMID: 18558656.

Kõressaar, T., Lepamets, M., Kaplinski, L., Raime, K., Andreson, R., and Remm, M. 2018. Primer3-masker: integrating masking of template sequence with primer design software. Bioinformatics, **34**: 1937–1938. Available at:. doi:10.1093/bioinformatics/bty036. PMID: 29360956.

Lutts, S., Ndikumana, J., and Louant, B.P. 1991. Fertility of *Brachiaria ruziziensis* in interspecific crosses with *Brachiaria decumbens* and *Brachiaria brizantha*: meiotic behaviour, pollen viability and seed set. Euphytica, **57**: 267–274. Available at:. doi:10.1007/BF00039673.

Melo, J.R., and Dawe, R.K. 2004. *Tripsacum dactyloides clone CentT57 centromeric repeat sequence* [GenBank: AY643032.1]. Available from https://www.ncbi.nlm.nih.gov/nuccore/49425120 [accessed 22 February 2023].

Melters, D.P., Bradnam, K.R., Young, H.A., Telis, N., May, M.R., Ruby, J.G., et al. 2013. Comparative analysis of tandem repeats from hundreds of species reveals unique insights into centromere evolution. Genome Biol. **14**: 1–20. doi:10.1186/gb-2013-14-1-r10.

Mendes-Bonato, A.B., Filho, R.G.J., Pagliarini, M.S., Do Valle, B.C., and De Penteado, M.I.O. 2002a. Unusual cytological patterns of microsporogenesis in Brachiaria decumbens: abnormalities in spindle and defective cytokinesis causing precocious cellularization. Cell Biol. Int. **26**: 641–646. doi:10.1006/cbir.2002.0929. PMID: 12127944.

Mendes-Bonato, A.B., Pagliarini, M.S., Forli, F., Borges Do Valle, C., and De Oliveira Penteado, M.I. 2002b. Chromosome numbers and microsporogenesis in *Brachiaria brizantha* (Gramineae). Euphytica, **125**: 419–425. Available at:. doi:10.1023/A:1016026027724.

Mendes-Bonato, A.B., Risso-Pascotto, C., Pagliarini, M.S., and Valle, C.B. 2006. Cytogenetic evidence for genome elimination during microsporogenesis in interspecific hybrid between *Brachiaria ruziziensis* and *B. brizantha* (Poaceae). Genet. Mol. Biol. **29**: 711–714. doi:10.1590/S1415-47572006000400021.

Meyers, B.C., Tingey, S.V., and Morgante, M. 2001. Abundance, distribution, and transcriptional activity of repetitive elements in the maize genome. Genome Res. **11**: 1660–1676. doi:10.1101/gr.188201. PMID: 11591643.

Miura, A., Yonebayashi, S., Watanabe, K., Toyama, T., Shimada, H., and Kakutani, T. 2001. Mobilization of transposons by a mutation abolishing full DNA methylation in *Arabidopsis*. Nature, **411**(6834): 212–214. doi:10.1038/35075612. PMID: 11346800.

Moraes, IDeC, Pereira, W.A., Nani, T.F., Paula, CMPDe, Rocha, MJDa, Souza Sobrinho, F., and Techio, V.H. 2021. Karyotype analysis and mode of reproduction of two species of *Urochloa* P. Beauv. Crop Sci. **61**: 3415–3424. doi:10.1002/csc2.20542.

Nani, T.F., Pereira, D.L., Souza Sobrinho, F., and Techio, V.H. 2016. Physical map of repetitive DNA sites in *Brachiaria* spp.: intravarietal and interspecific polymorphisms. Crop Sci. **56**: 1769–1783. doi:10.2135/cropsci2015.12.0760.

Nani, T.F., Schnable, JC., Washburn, JD., Albert, P., Pereira, W.A., Sobrinho, F.S., et al. 2018. Location of low copy genes in chromosomes of *Brachiaria* spp. Mol. Biol. Rep. **45**: 109–118. doi:10.1007/s11033-018-4144-5. PMID: 29330722.

Neumann, P., Novák, P., Hoštáková, N., and MacAs, J. 2019. Systematic survey of plant LTR-retrotransposons elucidates phylogenetic relationships of their polyprotein domains and provides a reference for element classification. Mobile DNA, **10**: 1–17. doi:10.1186/s13100-018-0144-1. PMID: 30622655.

Novák, P., Neumann, P., Pech, J., Steinhaisl, J., and MacAs, J. 2013. RepeatExplorer: a galaxy-based web server for genome-wide characterization of eukaryotic repetitive elements from next-generation sequence reads. Bioinformatics, **29**: 792–793. doi:10.1093/bioinformatics/btt054. PMID: 23376349.

Novák, P., Ávila Robledillo, L., Koblížková, A., Vrbová, I., Neumann, P., and Macas, J. 2017. TAREAN: a computational tool for identification and characterization of satellite DNA from unassembled short reads. Nucleic Acids Res. **45**: e111–e111. doi:10.1093/nar/gkx257.

Oliveira, L.C., and Torres, G.A. 2018. Plant centromeres: genetics, epigenetics and evolution. Mol. Biol. Rep. **45**: 1491–1497. doi:10.1007/s11033-018-4284-7. PMID: 30117088.

Pinto De Paula, C.M., Sobrinho, F.S., and Techio, V.H. 2017. Genomic constitution and relationship in *Urochloa* (Poaceae) species and hybrids. Crop Sci. **57**: 2605–2616. doi:10.2135/cropsci2017.05.0307.

Penteado, M.I.O., et al. 2000. Determinação de poliploidia e avaliação da quantidade de DNA total em diferentes espécies do gênero *Brachiaria*. Boletim de Pesquisa Embrapa, **11**.

Pessoa-Filho, M., Martins, A.M., and Ferreira, M.E. 2017. Molecular dating of phylogenetic divergence between *Urochloa* species based on complete chloroplast genomes. BMC Genomics, **18**, p. 516. doi:10.1186/s12864-017-3904-2. PMID: 28683832.

Renvoize, S., and Maass, B. 1993. *Brachiaria*: A report to CIAT, Colombia, on the species and specimens held in the germplasm collection. Kew: Royal Botanic Gardens.

Renvoize, S.A., Clayton, W.D., and Kabuye, C.H. 1996. Morphology, taxonomy, and natural distribution of *Brachiaria* (Trin.) Griseb.

Ricci, G.C.L., Souza-Kaneshima, A.M.D., Felismino, M.F., Mendes-Bonato, A.B., Pagliarini, M.S., and VALLE, C.B.D. 2011. Chromosome numbers and meiotic analysis in the pre-breeding of *Brachiaria decumbens* (Poaceae). J. Genet. **90**: 289–294. doi:10.1007/s12041-011-0087-5. PMID: 21869477.

da Rocha, M.J., Chiavegatto, R.B., Damasceno, A.G., Rocha, L.C., Souza Sobrinho, F., and Techio, V.H. 2019. Comparative meiosis and cytogenomic analysis in euploid and aneuploid hybrids of *Urochloa* P. Beauv. Chromosome Res. **27**: 333–344. doi:10.1007/s10577-019-09616-y.

Ruiz-Ruano, F.J., López-León, M.D., Cabrero, J., and Camacho, J.P.M. 2016. High-throughput analysis of the satellitome illuminates satellite DNA evolution. Scientific Rep. **6**. 28333. doi:10.1038/srep28333. PMID: 27385065.

Santos, F.C., Guyot, R., Do Valle, C.B., Chiari, L., Techio, V.H., Heslop-Harrison, P., and Vanzela, A.L.L. 2015. Chromosomal distribution and evolution of abundant retrotransposons in plants: gypsy elements in diploid and polyploid *Brachiaria* forage grasses. Chromosome Res. **23**: 571–582. doi:10.1007/s10577-015-9492-6. PMID: 26386563.

Smit, A.F.A., Hubley, R., and Green, P. 2020. RepeatMasker 4.1.1. Available from http://www.repeatmasker.org/ [accessed 22 January 2022].

Su, H., Liu, Y., Liu, C., Shi, Q., Huang, Y., and Han, F. 2019. Centromere satellite repeats have undergone rapid changes in polyploid wheat subgenomes. Plant Cell, **31**(9): 2035–2051. doi:10.1105/tpc.19.00133.

Tomaszewska, P., Pellny, T.K., Hernández, L.M., Mitchell, R.A.C., Castiblanco, V., De Vega, J.J., et al. 2021. Flow cytometry-based determination of ploidy from dried leaf specimens in genomically complex collections of the tropical forage grass *Urochloa* sl. Genes, **12**, p. 957. doi:10.3390/genes12070957. PMID: 34201593.

Tomaszewska, P., Vorontsova, M.S., Renvoize, S.A., Ficinski, S.Z., Tohme, J., Schwarzacher, T., et al. 2023. Complex polyploid and hybrid species in an apomictic and sexual tropical forage grass group: genomic composition and evolution in *Urochloa* (*Brachiaria*) species. Ann. Bot. **131**: 87–108. doi:10.1093/aob/mcab147.

Triviño, N.J., Perez, J.G., Recio, M.E., Ebina, M., Yamanaka, N., Tsuruta, S.-I., et al. 2017. Genetic diversity and population structure of *Brachiaria* species and breeding populations. Crop Sci. **57**: 2633–2644. doi:10.2135/cropsci2017.01.0045.

Valle, C.B., and Pagliarini, M.S. 2009. Biology, cytogenetics, and breeding of *Brachiaria*. *In* Genetic resources, chromosome engineering, and crop improvement, *Edited by* R.J. Singh. CRC Press. Boca Raton. pp. 103–143.

Vicient, C.M., Jaaskelainen, M.J., Kalendar, R., and Schulman, A.H. 2001. Active retrotransposons are a common feature of grass genomes. Plant Physiol. **125**(3): 1283–1292. doi:10.1104/pp.125.3.1283. PMID: 11244109.

Wang, Y., Xu, Z., and Guo, X. 2001. A centromeric satellite sequence in the Pacific oyster (Crassostrea gigas Thunberg) identified by fluores-

cence in situ hybridization. Mar. Biotechnol. **3**: 486–492. doi:10.1007/s10126-001-0063-3. PMID: 14961342.

Wicker, T., Guyot, R., Yahiaoui, N., and Keller, B. 2003. CACTA transposons in Triticeae: a diverse family of high-copy repetitive elements. Plant Physiol. **132**: 52–63. doi:10.1104/pp.102.015743. PMID: 12746511.

Wicker, T., Schulman, A.H., Tanskanen, J., Spannagl, M., Twardziok, S., Mascher, M., et al. 2017. The repetitive landscape of the 5100 mbp barley genome [online]. Mobile DNA, **8**: 1–16. doi:10.1186/s13100-017-0102-3. PMID: 28096902.

Worthington, M., Perez, J.G., Mussurova, S., Silva-Cordoba, A., Castiblanco, V., Cardoso Arango, J.A., et al. 2021. A new genome allows the identification of genes associated with natural variation in aluminium tolerance in *Brachiaria* grasses. J. Exp. Bot. **72**: 302–319. doi:10.1093/jxb/eraa469. PMID: 33064149.